[redacted] STATINTL

26 June 1964
RK:bb:283
Revised 7/9/64

STATINTL

MEMORANDUM FOR THE RECORD

By: [redacted]

Subject: Results of Theoretical Studies of the Influence of the Degree of STATINTL Coherence Upon Images of Edges

CC: [redacted]

INTRODUCTION

This memo reports the results to date of experimental and theoretical research investigating the influences of the degree of coherence of the illumination upon the formation of images in optical systems. Previous research[1] in this area has been limited to the study of "sine-wave" objects. Investigations, which are reported in this paper, deal with "edge" and rectangular objects. Although different portions of this work were conducted under each of two current projects (Microcap and Internal Research 86-139), this joint memo was prepared because of common objects. The theoretical studies of single edges and rectangular objects were completed under the Internal Research. The computer computations for the rectangular objects, as well as the investigations relating to trapezoidal objects and to the illuminating microscope, were carried out under Microcap.

BACKGROUND

STATINTL

General coherence theory, presented in detail by [redacted][2] deals not only with completely coherent or incoherent illumination but with partially coherent illumination as well. Within the structure of the theory, coherence and incoherence represent limiting cases. In the study of partial coherence it is expedient to eliminate some mathematical complexity of the general theory by restricting the class of optical systems investigated to those in which the usual "small angle approximation" is

STATINTL

1 [redacted] Proc. Roy. Soc. A217 408 1953

2 [redacted] Principles of Optics Chapter 10 Pergamon Press 1959

STATINTL

valid. The coherence of the light in a plane, say the x , y plane, of such an optical system is expressed through $\Gamma(x_1, x_2, y_1, y_2)$, the mutual intensity function. This function is defined in terms of the correlation of the light signals at two points, (x_1 , y_1) and (x_2 , y_2) in the x, y plane (see Reference 2, p. 504).

Consider two successive planes in an optical system which have the property that translation of an object or a stop in the first plane has no influence upon the intensity distribution in the second plane except for differences caused by differences in illumination of the first plane. In a spatial filtering apparatus, for example, the object plane and filter plane are two such planes. Planes that possess this property will be called relatively Fraunhofer.

It can be shown* that the propagation of the mutual intensity between successive planes that are relatively Fraunhofer is given by:

$$\Gamma(x_1, x_2) = K \iint \Gamma(\xi_1, \xi_2)\, e^{i(x_2\xi_2 - x_1\xi_1)}\, d\xi_1 d\xi_2 \qquad (1)$$

Consider the optical system consisting of four successive, relatively Fraunhofer planes shown in Figure 1. The Fourier or lens plane, in addition to being relatively Fraunhofer with respect to the object plane, also contains the aperture stop of the imaging section.

TYPICAL OPTICAL SYSTEM

FIGURE 1

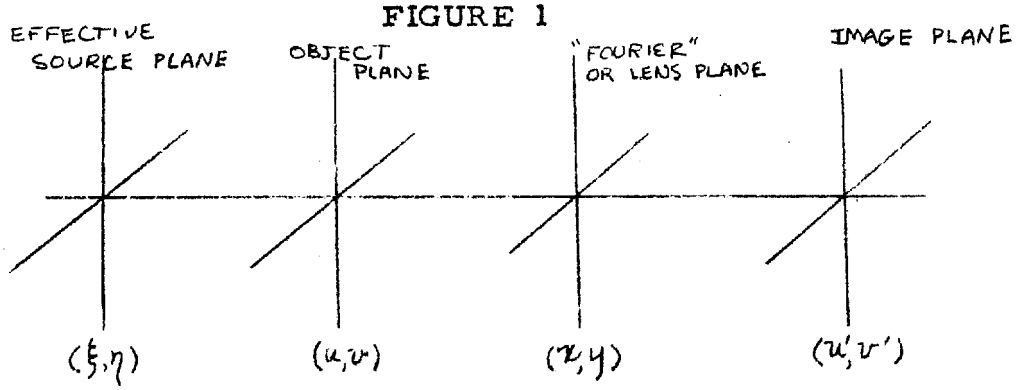

STATINTL

STATINTL

* This was demonstrated to the author by [redacted] and is a stated result which can be found in one-dimensional form in AF CRL-64-19, "Mutual Coherence and the Array Theorem", [redacted] Laboratories, p. 6.

In an actual optical system the effective source plane need not exist, and it is introduced in the theory only as a mathematical convenience. The coherence condition of the light illuminating the object plane (u , v plane) can be described by imagining an effective source to exist in the ξ , η plane which has an area A (ξ , η) and a mutual intensity function $\Gamma_s(\xi_1, \xi_2, \eta_1, \eta_2)$. The subsequent mutual intensity function in the object plane is determined by the two-dimensional form of Equation (1) and is:

$$\Gamma_o(u_1, u_2, v_1, v_2) = K \iiiint \Gamma_s(\xi_1, \xi_2, \eta_1, \eta_2)\, e^{i(u_2\xi_2 - u_1\xi_1 + v_2\eta_2 - v_1\eta_1)}\, d\xi_1 d\xi_2 d\eta_1 d\eta_2 \qquad (2)$$

By restricting the effective source to be incoherent over its entire area one has:

$$\Gamma_s(\xi_1, \xi_2, \eta_1, \eta_2) = A(\xi, \eta)\, \delta(\xi_1 - \xi_2)\, \delta(\eta_1 - \eta_2)$$

OR

$$\Gamma_o(u_1 - u_2, v_1 - v_2) = K \iint A(\xi, \eta)\, e^{i[(u_2 - u_1)\xi + (v_2 - v_1)\eta]}\, d\xi d\eta \qquad (3)$$

STATINTL

STATINTL

This is the relationship which is the basis of a method of analysis employed by [redacted] to study partially coherent illumination. It relates the area of the effective source to the coherence properties of the light illuminating an object by a Fourier transform. It should be pointed out that by assuming the "effective" source is a bounded incoherent source that the light which illuminates the object must be characterized by a spatially stationary mutual intensity function.** By tracing the mutual intensity function from one relatively Fraunhofer plane to the next through the complete optical system (see Figure 1), the intensity in the image plane*** can be derived in terms of

---

* The object is assumed to be uniformly illuminated so that $K = 2\pi$.

** The degree to which this requirement limits the applicability of the theory to some optical systems is a question not answered by myself.

*** The intensity in the image plane is found by computing the mutual intensity function, $\Gamma(u_1', u_2', v_1', v_2')$, and allowing $u_1' = u_2' = u'$ and $v_1' = v_2' = v'$.

STATINTL

a six-dimensional integral equation. This multiple integral equation is derived by [redacted] using a slightly different approach. The various integrations may be grouped in several ways. One way involves the integration of the product of the effective source area, $A(x, y)$, and the complex transmittance of the lens aperture, $\S(x, y)$, evaluated at two points in the Fourier plane to form a four-dimensional transfer function, $c(m,n,p,q)$.*

$$c(m,n,p,q) = 2\pi \iint_{-\infty}^{\infty} A(x,y)\,\S(x+m,y+n)\,\S^{*}(x+p,y+q)\,dx\,dy \tag{4}$$

Once $c(m,n,p,q)$ is known, the intensity distribution in the image plane is determined by the multiple integral:

$$I'(u') = \left(\frac{1}{2\pi}\right)^{2} \iiiint c(m,n,p,q)\,O(m,n)\,O^{*}(p,q)\,e^{i[(m-p)u'+(n-q)v']}\,dm\,dn\,dp\,dq \tag{5}$$

where the O-function is the complex Fourier Spectrum of the object, and it is evaluated at two different frequencies. This approach is useful when investigating a fixed or particular optical system for varying objects since $c(m,n,p,q)$ remains a fixed function and also has the advantage of yielding a function which can be interpreted as a system "transfer function". Another way to group the various integrations is to integrate the product of the object spectrum and complex transmittance over the "frequency" or Fourier plane. This integration yields

$$\Phi(x,y,u',v') = \frac{1}{2\pi} \iint O(m,n)\,\S(x+m,y+n)\,e^{i(mu'+nv')}\,dm\,dn \tag{6}$$

The subsequent intensity distribution in the image plane is determined by the multiple integrals:

$$I'(u') = 2\pi \iint A(x,y)\,|\Phi(x,y,u',v')|^{2}\,dx\,dy \tag{7}$$

STATINTL

---

[3] [redacted] loc. cit.

* The magnification between the effective source plane and the Fourier plane is assumed to be unity so $\xi = x$ and $\eta = y$.

This approach has the advantage of being useful in varying the degree of coherence illuminating a fixed object imaged by a particular imaging system. Consequently, it would seem that this approach would be well suited to the investigation of the influence of coherence upon edges and other objects. Both of these approaches have been employed in the investigation of edge objects.

COORDINATES AND SCALE FACTORS

Before discussing the results which have been achieved, it should be pointed out that the u, v, u', and v' coordinates appearing in the equations are not the geometrical coordinates of the optical system. These coordinates will be called reduced coordinates. They are related to the geometrical coordinates u_o, v_o, u_o', and v_o' by the following relationship.

$$(\text{Coordinate})_o = \left(\frac{\text{Reduced}}{\text{Coordinate}}\right) / k \times (\text{Numerial Aperture})$$

where k is the wave number.
It can be seen that the reduced coordinates are dimensionless. The table below presents some scale factors for various numerical apertures in the [redacted] microdensitometer and for the spatial filtering apparatus.

STATINTL

TABLE
SCALE FACTORS

Instrument	Number of Microns Corresponding to One Reduced Unit
Microdensitometer	
N.A. = 0.1	1.75
N.A. = 0.25	0.35
N.A. = 0.40	0.22
Spatial Filtering	5.00 (3/4" Aperture in Filter Plane)

Incoherent and Coherent Limits

As examples of effective sources, the limits of complete coherence and complete incoherence will be demonstrated. For the object to be illuminated completely

incoherently, the mutual intensity function $\Gamma(u_1, u_2, v_1, v_2)$ must be given by:

$$\Gamma(u_1, u_2, v_1, v_2) = \delta(u_1 - u_2, v_1 - v_2)$$

and therefore from the inverse transform of Equation (3) the effective source representing the incoherent limit becomes:

$$A(x, y) = \frac{1}{2\pi} \quad \text{for all } x, y \tag{8}$$

Similarly, for completely coherent illumination (i.e. $\Gamma(u_1, u_2, v_1, v_2) = 1$ for all u_1, u_2, v_1 and v_2) the effective source becomes:

$$A(x, y) = \frac{1}{2\pi} \delta(x - x_0, y - y_0) \tag{9}$$

Application to Microdensitometer System

The analysis which is reported in this memo is primarily concerned with the imaging section of the optical system shown in Figure 1. In the microdensitometer the Fourier plane is assumed to be the plane of the objective of the analytical microscope and an addition to the system shown in the figure is a scanning aperture behind the image plane. Throughout the analysis, it is assumed that the area of the image is large compared to the scanning aperture which is the mode of operation usually recommended by the manufacturer. Another assumption that is made for ease in analysis is that the optics contained in the imaging section are aberration free.

Transfer Function Approach

Initial investigations were carried out using the approach employing expressions (4) and (5). The coherence condition imposed was that the area of the effective source was such as to just fill the aperture in the Fourier plane. This case occurs when the numerical apertures of the illuminating and analytical objectives are equal, which is the normal method of operation in the [redacted] microdensitometer. As a result, the "transfer function" (i.e., Equation (14)) becomes:*

$$c(m, n, p, q) = \iint f(x, y) f(x+m, y+n) f^*(x+p, y+q)\, dx\, dy$$

STATINTL

* Substitute $A(x, y) = \frac{1}{2\pi} f(x, y)$ into Equation (4).

which, for one-dimensional objects, may be reduced to:

$$C(m,p) = \iint f(x,y)\, f(x+m,y)\, f^*(x+p,y)\, dx\, dy$$

when:

$$f(x,y) = \begin{cases} 1 & \sqrt{x^2+y^2} \le 1 \\ 0 & \text{otherwise} \end{cases}$$

A sketch of $C(m,p)$ is shown in Figure 2.

FIGURE 2

$C(m,p)$ - CIRCULAR APERTURE

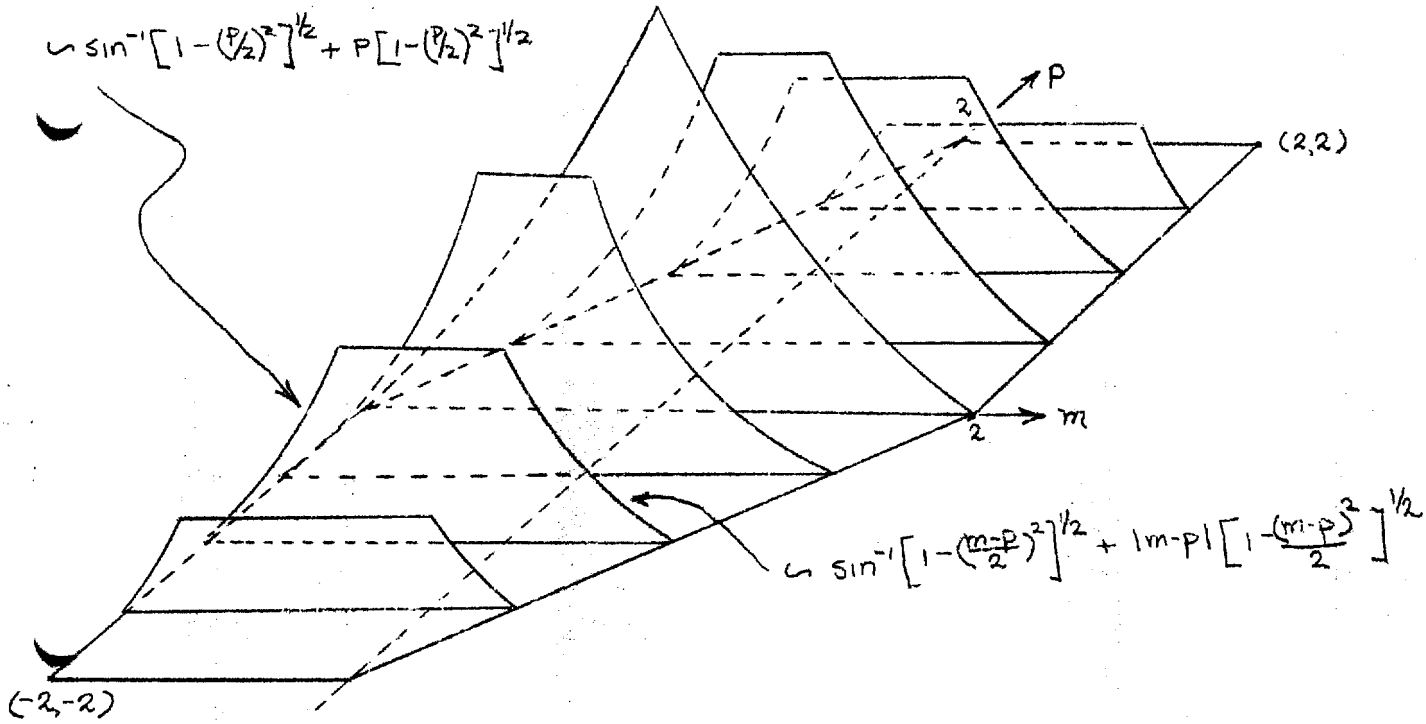

This approach was not examined beyond this point for several reasons. $C(m,p)$ is not a closed functional form making the integrations of expression (5) difficult and it does not facilitate the examination of many degrees of coherence.

ALTERNATE APPROACH

Single Edge

When employing the second approach outlined earlier, a specific object must be chosen. The first object examined was that of a single edge described by the amplitude transmittance:

$$T(u,v) = \begin{cases} A_0 & u>0,\ |v|<\infty \\ \frac{A_0}{2} & u=0,\ |v|<\infty \\ 0 & u<0,\ |v|<\infty \end{cases} \tag{10}$$

The Amplitude Fourier Spectrum of this object is given by:

$$O(m,n) = \frac{1}{2\pi} \int T(u,v)\, e^{i(mu+nv)}\, du\, dv$$

which upon substitution of $T(u,v)$ from 10 becomes:*

$$O(m,n) = A_0\, \delta(n) \left\{ \pi\, \delta(m) + \frac{1}{im} \right\} \tag{11}$$

This is then substituted into Equation (6) to determine the ϕ -function,

$$\Phi(x,y,u',v') = \frac{A_0}{2\pi} \int\int \delta(n) \left\{ \pi\, \delta(m) + \frac{1}{im} \right\} f(x+m, y+n)\, e^{i(mu'+nv')}\, dm\, dn$$

the integration over n may be done immediately to yield

$$\Phi(x,y,u') = \frac{A_0}{2\pi} \int \left\{ \pi\, \delta(m) + \frac{1}{im} \right\} f(x+m, y)\, e^{imu'}\, dm$$

Letting $f(x,y)$ represent a square aperture

$$f(x+m,y) = \begin{cases} 1 & -B-x \le m \le B-x,\ |y| \le B \\ 0 & \text{elsewhere} \end{cases} \tag{12}$$

and expanding the exponential term:

$$\phi(x,y,u') = \frac{A_0}{2\pi} \left\{ \pi f(x,y) + \int_{-B-x}^{B-x} \frac{\sin mu'}{m} dm - i \int_{-B-x}^{B-x} \frac{\cos mu'}{m} dm \right\}$$

which is integrable in terms of sine and cosine integral functions, Si and Ci . The result for $|\phi(x,y,u')|^2$ is:

$$|\phi(x,y,u')|^2 = \frac{I_0}{4\pi^2} \left\{ \left[\pi f(x,y) + Si(B+x)u' + Si(B-x)u' \right]^2 + \left[Ci(B+x)u' - Ci(B-x)u' \right]^2 \right\} \tag{13}$$

Note that: $|y| \le B$ otherwise $|\Phi(x,y,u')|^2 = 0$.

---

* For the evaluation of this integral, see [redacted] "Fourier Analysis and Generalized Function", Cambridge University Press, 1960, p. 43.

STAT INTL

One can allow B = 1 without any loss in generality and this will be done in the following analysis. This expression is substituted into (7) along with the appropriate area of the effective source to find the image intensity for varying degrees of coherence. Consider the coherent limit where the effective source is given by Equation (9). Expression (7) becomes:

$$I'(u') = |\Phi(x_0, y_0, u')|^2 \qquad |y_0| \le 1$$

$$= \frac{I_0}{4\pi^2}\left\{\left[\pi f(x_0,y_0) + Si(1+x_0)u' + Si(1-x_0)u'\right]^2 + \left[Ci(1+x_0)u' - Ci(1-x_0)u'\right]^2\right\} \qquad (14)$$

where $$f(x_0,y_0) = \begin{cases} 1 & \text{for } |x_0| \le 1,\ |y_0| \le 1 \\ 0 & \text{otherwise} \end{cases}$$

Physically, different values of (x_0, y_0) represent different incident angles between the object plane and the illuminating plane wave. Since the image intensity I' is independent of y_0 , if $|y_0| \le 1$, it is instructive to examine the change in I' as x_0 is varied. Several computations were made for x_0 = 0, 0.5, 0.98, 1.01, 1.02, 1.10.* The intensity ($I'(u') \cdot \frac{4\pi^2}{I_0}$) versus position (u') curves are plotted in Figure 3.** Several hypotheses can be made about less coherent illumination by examining the figure. Note that the only essential difference between the $x_0 = 0$ and $x_0 = 0.5$ curves is decreased in ringing at the top of the edge. This observation can be made for all $x_0 \le 0.9$, although it is not shown in the figure. Consequently, an effective source which extended from $x_0 = -0.9$ to $x_0 = +0.9$ should produce little change in the edge gradient. However, when $0.9 \le |x_0| \le 1.0$, the coherently illuminated edge shows a marked shift and increase in the level of intensity at the toe of the edge. Consequently, one would expect that the extension of the effective source to an area represetned by $x_0 = -1.0$ to $x_0 = 1.0$ would decrease the contrast of the edge and also produce a smaller edge gradient. Further extension of the effective spurce (i.e., less coherence) will add intensity distributions similar to those shown in the lower curves. The effect of this extension appears to be additional

* When the values of argument are small, it must be recalled that $Ci(x) \sim \ln \gamma x$ in order to perform the proper numerical evaluation.

** Also shown in Figure 3 is the incoherent limit which was determined by convolving the intensity distribution of the object with the imaging system point spread. This limit could also be reached by using an effective source given by expression (8) in expression (7). However, it appears the resulting integration must be done numerically and therefore is impractical.

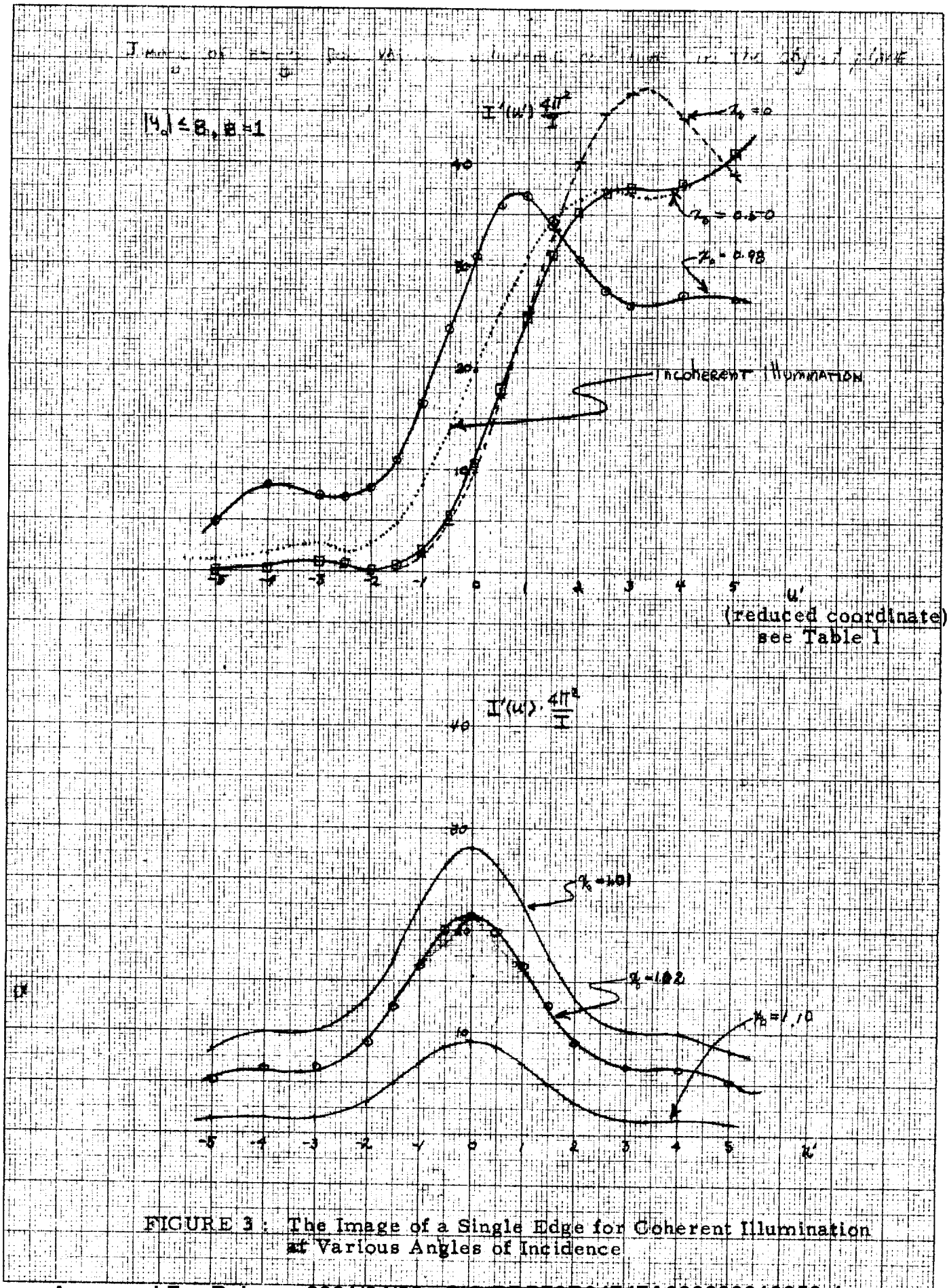

FIGURE 3 : The Image of a Single Edge for Coherent Illumination at Various Angles of Incidence

loss in edge gradient. These conclusions can be tested by performing the integrations in expression (7) for various effective sources. Assuming $A(x,y)$ is:

$$A(x,y) = \begin{cases} \frac{1}{2\pi} & |x| \le \epsilon \,,\ |y| \le \epsilon \\ 0 & \text{otherwise} \end{cases}$$

and using expression (13) for $|\Phi(x,y,w')|^2$ Equation (7) becomes:

$$I'(w') = \frac{I_0}{4\pi^2}\left[4\pi^2\epsilon^2 + 4\pi\epsilon \int_{-\epsilon}^{\epsilon} \left\{Si(1+x)w' + Si(1-x)w'\right\} dx + 2\epsilon \int_{-\epsilon}^{\epsilon} \left\{\left[Si(1+x)w' + Si(1-x)w'\right]^2 + \left[Ci(1+x)w' - Ci(1-x)w'\right]^2\right\} dx\right]$$

where $\epsilon \le 1$

Unfortunately the second integral does not exist at $x = \pm 1$ since $Ci(1+x)w'$ or $Ci(1-x)w'$ diverge*, and therefore, the integration cannot be completed numerically for $\epsilon \ge 1$. This circumstance led to the investigation of rectangular objects.

Rectangular Object

Consider an object whose amplitude transmittance is:

$$T(u,v) = \begin{cases} A_0 & 0 < u < W,\ |v| < \infty \\ A_0/2 & u = 0,\ u = W,\ |v| < \infty \\ 0 & \text{otherwise} \end{cases} \qquad (15)$$

The amplitude Fourier Spectrum of this object is given by:

$$O(m,n) = 2A_0\,\delta(n)\,\frac{\sin\frac{mW}{2}}{m}\,e^{-i\frac{mW}{2}} \qquad (16)$$

Substitution of (15) and (16) into (6) yields:

$$\Phi(x,y,w') = \frac{A_0}{\pi}\left\{\int_{-\infty}^{\infty} \frac{\sin\frac{mW}{2}\cos m(w'-\frac{W}{2})}{m} f(x+m,y)\,dm + i\int_{-\infty}^{\infty} \frac{\sin\frac{mW}{2}\sin m(w'-\frac{W}{2})}{m} f(x+m,y)\,dm\right\}$$

* This problem was investigated by [redacted] who concluded that the divergent properties arose from the mathematical approach rather than from the unlimited energy of the object.

STATINTL

Letting $f(x,y)$ represent a square aperture as before, see expression (12), $|\Phi(x,y,u')|^2$ can be written as:

$$|\Phi(x,y,u')|^2 = \frac{I_0}{4\pi^2}\left\{\left[Re(\Phi)\right]^2 + \left[Im(\Phi)\right]^2\right\} \tag{17}$$

where

$$Re(\Phi) = \int_{-1-x}^{1-x} \frac{2\sin\frac{mw}{2}\cos m(u'-\frac{w}{2})}{m}\,dm$$

and

$$Im(\Phi) = \int_{-1-x}^{1-x} \frac{2\sin\frac{mw}{2}\cos m(u'-\frac{w}{2})}{m}\,dm$$

Evaluation of $Re(\Phi)$ and $Im(\Phi)$ may be done easily by using the following identities:

$$2\sin\tfrac{mw}{2}\sin m(u'-\tfrac{w}{2}) = \cos(u'-w)m - \cos u'm$$

$$2\sin\tfrac{mw}{2}\cos m(u'-\tfrac{w}{2}) = \sin u'm - \sin(u'-w)m$$

It is found that:

$$Re(\Phi) = \left\{Si(1-x)u' + Si(1+x)u' - Si(1-x)(u'-w) - Si(1+x)(u'-w)\right\} \tag{17a}$$

$$Im(\Phi) = \left\{Ci(1+x)u' - Ci(1-x)u' + Ci(1-x)(u'-w) - Ci(1-x)(u'-w)\right\} \tag{17b}$$

where W is the width of the rectangular object.

Consider an effective source given by:

$$A(x,y) = \begin{cases} \frac{1}{2\pi} & |x|\le\epsilon\,,\ |y|\le 1 \\ 0 & \text{otherwise} \end{cases}$$

The source size, which depends on the value of ϵ, represents a particular mutual intensity function before the object plane. As ϵ approaches ∞ the incoherent limit is reached. Substitution of this effective source and expression (17) for $|\Phi(x,y,u')|^2$ into (7) yields an image intensity given by:

$$I'(u') = \frac{I_0}{4\pi^2}\int_{-\epsilon}^{\epsilon}\int_{-1}^{1}\left\{\left[Re(\Phi)\right]^2 + \left[Im(\Phi)\right]^2\right\}dx\,dy$$

Since $Re(\Phi)$ and $Im(\Phi)$ are independent of u_f :

$$I'(u') = \frac{I_o}{\pi^2}\left\{\int_0^{\epsilon}\left[Si(1-x)u' + Si(1+x)u' - Si(1-x)(u'-w) - Si(1+x)(u'-w)\right]^2 dx + \int_0^{\epsilon}\left[Ci(1+x)u' - Ci(1-x)u' + Ci(1-x)(u'-w) - Ci(1-x)(u'-w)\right]^2 dx\right\} \quad (18)$$

The evaluation of expression (18) required numerical integration and consequently a program was written for the IBM 704.* Before presenting the results of the computer evaluation, a physical interpretation of the value of ϵ in the microdensitometer will be discussed. The value of ϵ represents the relative size of the effective source compared to the aperture stop in the Fourier plane. When $\epsilon = 1$, the effective source just fills the aperture. Therefore, in the microdensitometer ϵ may be interpreted to be the ratio of the numerical aperture of the illumination objective to the numerical aperture of the analytical objective.

The computer program for the rectangular object was run for several object widths, in particular W=3000, 600, 300, 60 and 30 (in u'-units, see Table 1). Each object has been evaluated for ϵ values of 0.2, 0.4, 0.6, 0.8, 0.9, 0.95, 1.00, 1.05, 1.10, 1.20, 1.40 and 1.50. The relative intensity vs. position curves for image when W=3000 (u'-units) is shown in Figure 4. In order to compare the results for different values of coherence (i.e. ϵ) for the same object and to compare various size objects, an appropriate normalization procedure must be employed. The criterion of equal energy content within each image is desirable but not convenient since this requires knowledge of the total area under the intensity-position curves. Instead, a nearly equivalent criterion is employed in which the intensity at $u' = \frac{W}{2}$ is set equal to 1.0. When this is done, the intensity-position curves for

* The details of the program will not be presented in this memo. The subroutines for the evaluation of sine and cosine integral functions are the only parts of the program which may be useful to others.

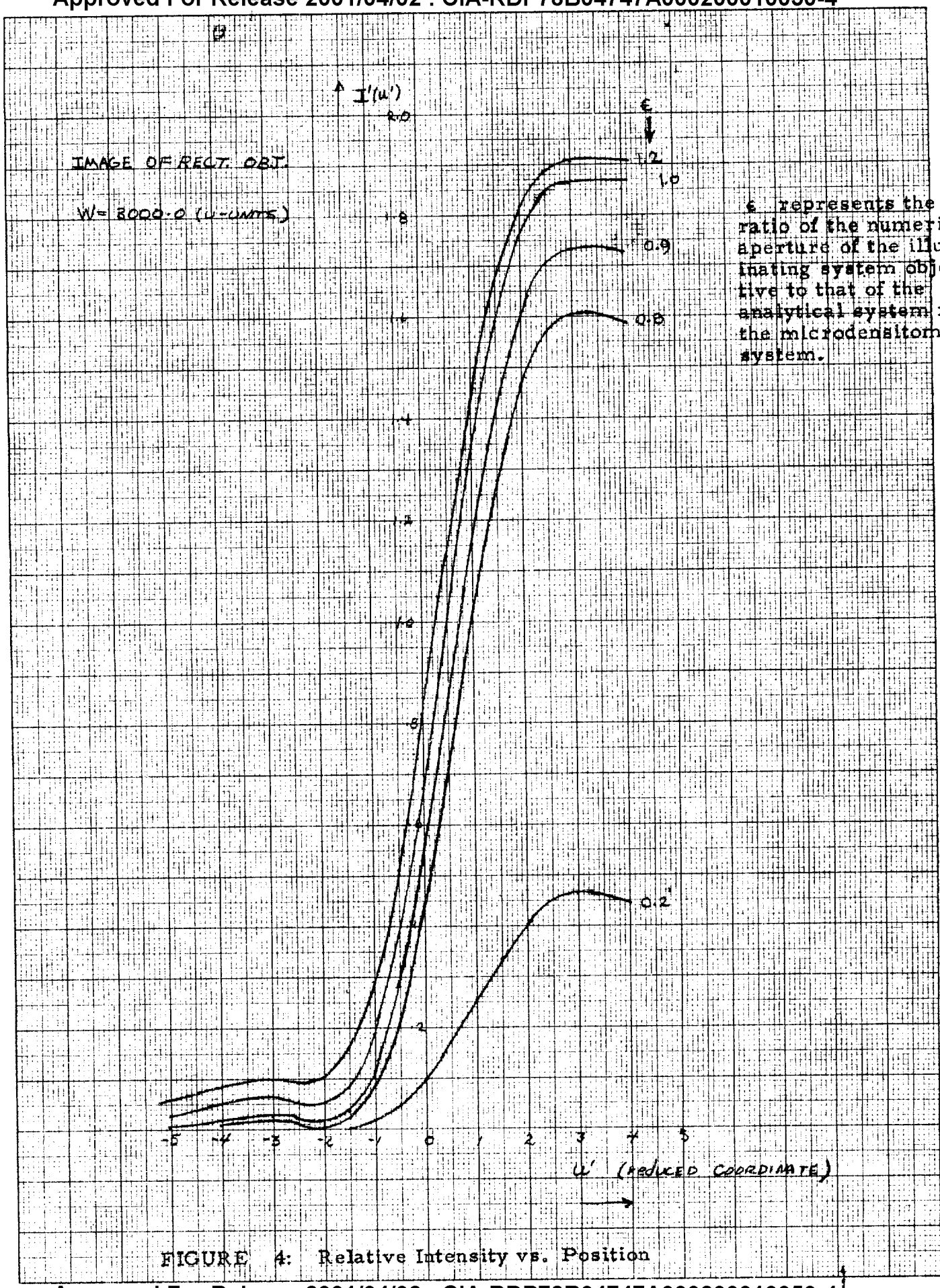

ε represents the ratio of the numerical aperture of the illuminating system objective to that of the analytical system for the microdensitometer system.

FIGURE 4: Relative Intensity vs. Position

all values of object width greater than 300 (u' -units) are practically identical. Figure 5 is a plot of these curves for various degrees of coherence. The effect of smaller object widths is currently being examined and will be reported in a future memo. Figure 5 exhibits some of the results which were suggested earlier in the memo. As ϵ changes from 0.2 to 0.9, the major change in the image of the edge is a decrease in the amount of "ringing" at the top of the image. However, as ϵ increases from 0.9 to 1.0, there is a significant increase in light levels of the toe of the image causing a reduction in contrast. Of course, the reduction is greater for high contrast objects. Further decrease in the degree of coherence (i.e. larger ϵ or overfilling the aperture) increases the loss of contrast. As ϵ approaches ∞ it appears that the incoherent limit is reached as expected. To examine the edge gradients Figure 6 is an expanded plot of the intensity-position curves for u' between -1.0 and 2.0. The table in the figure contains the value of edge gradient of a function of ϵ measured over the linear portion of each curve. It is evident that the gradient decreases with decreasing coherence (i.e. larger ϵ).

The conclusion drawn from these results is that it is possible for an edge image to possess a larger gradient without excess ringing when the ratio of the numerical aperture of the illuminating objective to that of the analytical objective is about 0.8 instead of 1.0 (i.e., matched apertures). The amount of improvement in a real system cannot be predicted because, in general, optical systems are not diffraction limited.

Other areas which have been briefly examined concerning imaging in the microdensitometer system includes: 1) Trapezoidal objects to account for a finite resolution of the object and 2) The influence of the size of the area illuminated upon the microdensitometer output.

TRAPEZOIDAL OBJECTS

The amplitude transmittance of the object in this case is assumed to be:

$$T(u) = \begin{cases} 0 & u \le 0 \\ \frac{Au}{S} & 0 \le u \le S \\ A & S \le u \le W+S \\ \frac{A}{S}(W+2S-u) & W+S \le u \le W+2S \\ 0 & W+2S \le u \end{cases} \tag{19}$$

The corresponding object spectrum is

$$O(m,n) = \frac{2A}{S}\,\delta(n)\left\{\frac{\cos\beta m - \cos\alpha m}{m^2}\right\} e^{-im\alpha} \tag{20}$$

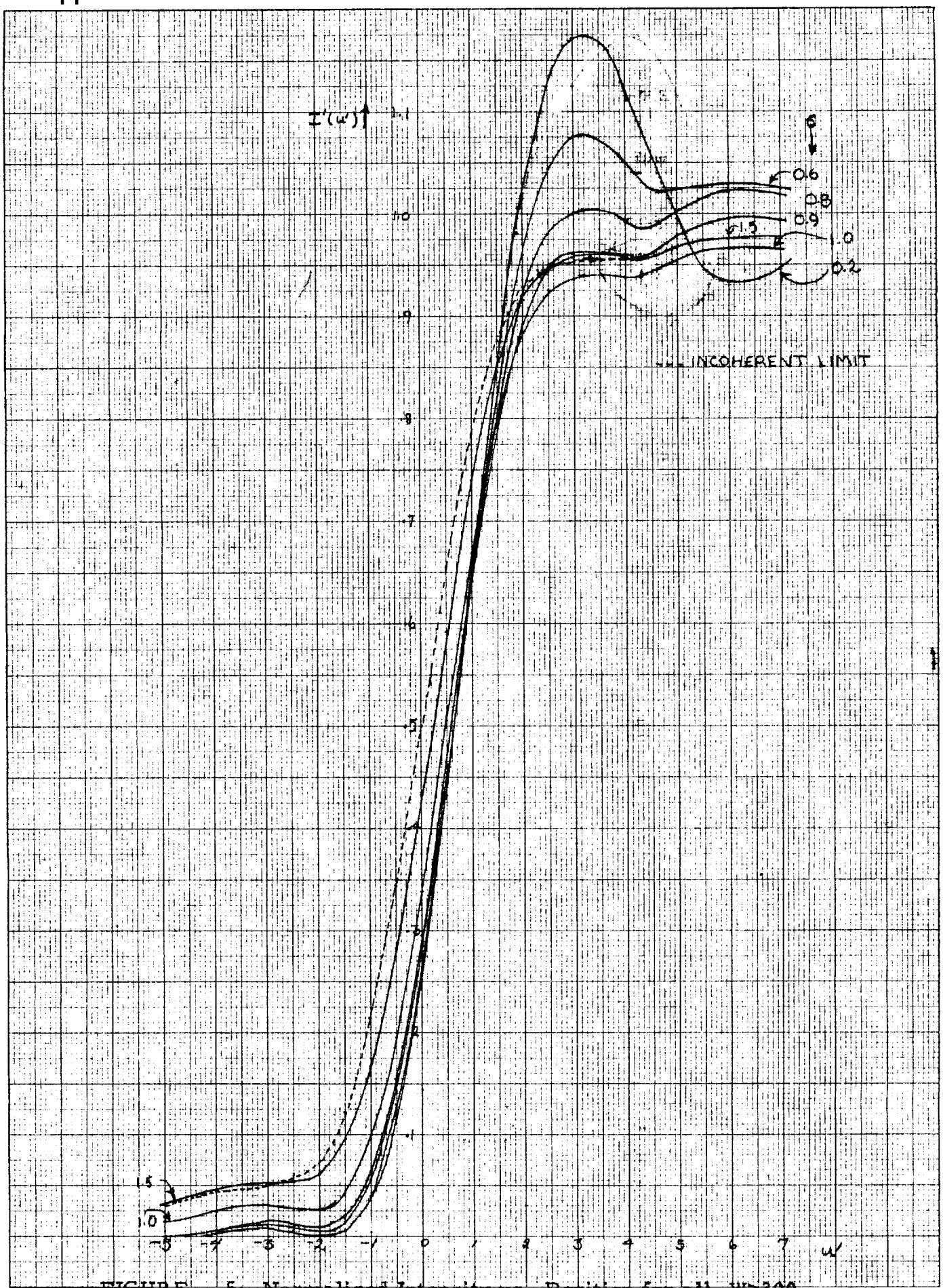

FIGURE 5. Normalized Intensity vs. Position for all W>300

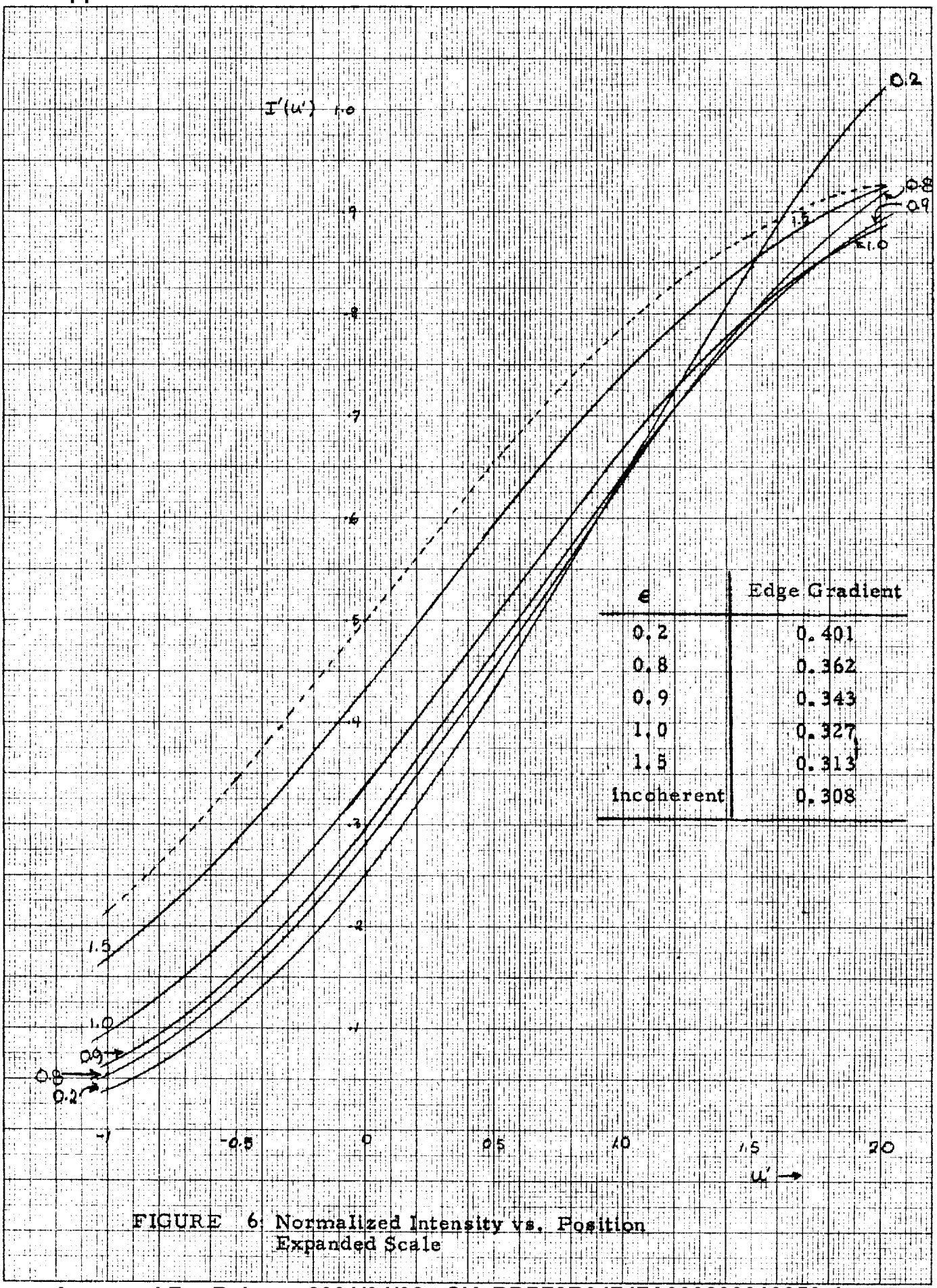

ϵ	Edge Gradient
0.2	0.401
0.8	0.362
0.9	0.343
1.0	0.327
1.5	0.313
Incoherent	0.308

FIGURE 6: Normalized Intensity vs. Position
Expanded Scale

where $\alpha = \frac{W}{2} + S$ and $\beta = W/2$

The value of $|\Phi(x,y,u')|^2$ is determined in the same way as before. A numerical evaluation of $I'(u')$ has not been programmed for the IBM 704 as yet.

INFLUENCE OF THE ILLUMINATING MICROSCOPE

The investigation of the limited area illuminating system is carried out from a slightly different theoretical approach than those described previously mainly because the theory of [redacted] assumed the entire object plane was uniformly illuminated. Figure (7) contains the optical system to be examined. All three planes are relatively Fraunhofer so that expression (1) may be used to propagate the mutual intensity function between each plane.

STATINTL

FIGURE 7

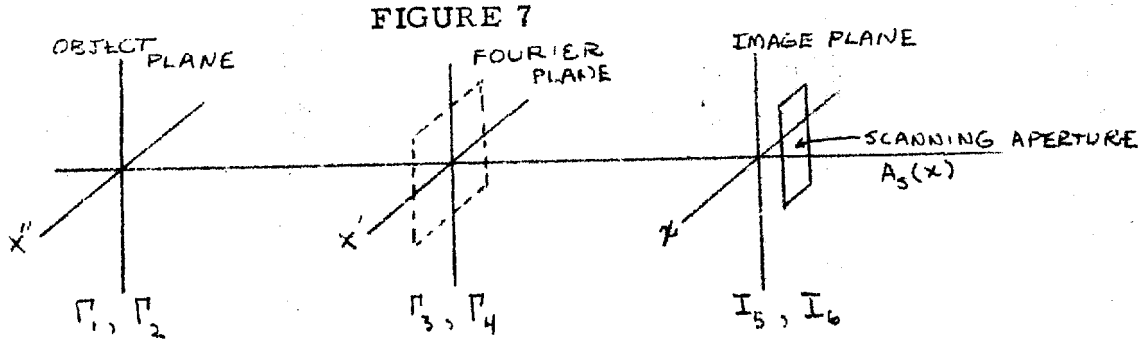

From expression (1) assuming $x_1 = x_2 = x$, the intensity in the image plane becomes:

$$I_5 = \iint \Gamma_4(x_1', x_2')\, e^{i(x_1' - x_2')x}\, dx_1'\, dx_2'$$

assume a clear aperture in the Fourier plane (i.e. system is aberration free) so:

$$\Gamma_4(x_1', x_2') = \begin{cases} \Gamma_3(x_1', x_2') & |x_1', x_2'| \le a \\ 0 & \text{otherwise} \end{cases}$$

and then:

$$I_5(x) = \int_{-a}^{a}\int \Gamma_3(x_1', x_2')\, e^{i(x_1' - x_2')}\, dx_1'\, dx_2' \qquad (21)$$

now again by employing expression (1):

$$\Gamma_3(x_1', x_2') = \iint \Gamma_2(x_1'', x_2'')\, e^{i(x_1'' x_1' - x_2'' x_2')}\, dx_1''\, dx_2'' \qquad (22)$$

In the microdensitometer the object is physically moved through the object plane so that the transmittance of the object (i.e. the area illuminated) is a function of time, therefore

$$\Gamma_2(x_1'', x_2'') = T(x_1'', t)\, T^*(x_2'', t)\, \Gamma_1(x_1'', x_2'')$$

since the mutual intensity function is modulated by the amplitude transmittance as it passes through the object. Combining this expression with (22) yields:

$$\Gamma_3(x_1', x_1') = \iint_{-\infty}^{\infty} T(x_1'', t) T^*(x_2'', t) \Gamma_1(x_1'', x_2'')\, e^{i(x_1'' x_1' - x_2'' x_2')}\, dx_1''\, dx_2''$$

this expression is now substituted into (21):

$$I_5(x, t) = \iint_{-a}^{a} \left[\iint_{-\infty}^{\infty} T(x_1'', t) T^*(x_2'', t) \Gamma_1(x_1'', x_2'') e^{i(x_1'' x_1' - x_2'' x_2')}\, dx_1''\, dx_2'' \right] e^{i(x_1' - x_2')\alpha}\, dx_1'\, dx_2'$$

by changing the order of integration, the integrations over x_1' and x_2' may be done to yield:

$$I_5(x, t) = \iint_{-\infty}^{\infty} T(x_1'', t) T^*(x_2'', t)\, \Gamma_1(x_1'', x_2'')\, \frac{\sin(x + x_1'')a}{x + x_1''} \cdot \frac{\sin(x + x_2'')a}{x + x_2''}\, dx_1''\, dx_2'' \qquad (23)$$

If the object is coherently illuminated then:

$$\Gamma_1(x_1'', x_2'') = \sqrt{I(x_1'')}\sqrt{I(x_2'')}$$

and (23) becomes

$$I_5(x, t) = \left\{ \int_{-\infty}^{\infty} \sqrt{I(x_1'')}\, T(x'', t)\, \frac{\sin(x + x'')a}{x + x''}\, dx'' \right\}^2 \qquad (23a)$$

For incoherent illumination

$$\Gamma_1(x_1'', x_2'') = \sqrt{I(x_1'')}\sqrt{I(x_2'')}\, \delta(x_1'' - x_2'')$$

and (23) becomes

$$I_5(x, t) = \int_{-\infty}^{\infty} I(x'')\, |T(x'', t)|^2 \left[\frac{\sin(x + x'')a}{x + x''} \right]^2 dx'' \qquad (23b)$$

Assume that the illuminating slit is a thin line so that the width of the illuminated area in the object plane is determined by the line spread of the illuminating systems' optics and the illumination is coherent. Now if the resolution limit of the illuminating and imaging systems are identical then:

$$\sqrt{I(x'')} = \sqrt{I_o}\ \frac{\sin ax''}{ax''}$$

This is substituted into expression (23a) to yield:

$$I_5(x,t) = I_o \left\{ \int_{-\infty}^{\infty} T(x',t)\ \frac{\sin(x+x'')a}{x+x''}\ \frac{\sin ax''}{ax''}\ dx'' \right\}^2 \qquad (24)$$

In order to investigat a rectangular object of width W, assume $T(x',t)$ to be given by:

$$T(x',t) = \begin{cases} 1 & x_o - st \le x'' \le x_o + w - st \\ 0 & \text{otherwise} \end{cases}$$

where x_o is the location of an edge of the object relative to the object plane when $t = o$. Substitution in (24) yields:

$$I_5(x,t) = I_o \left\{ \int_{x_o - st}^{x_o + w - st} \frac{\sin(x+x'')a}{x+x''}\ \frac{\sin ax''}{ax''}\ dx'' \right\}^2$$

A final step remains in computing the output of the microdensitometer and that is to include the influence of the aperture in the image plane. This accounted for by the following expression:

$$I_6(t) = \int_{-\infty}^{\infty} A_5(x)\, I_5(x,t)\, dx \qquad A_5(x) = \text{SCANNING APERTURE}$$

For convelence, assume that $A(x) = \delta(x)$ (i.e. a thin line aperture). This same assumption was made about the illuminating slit and therefore is reasonable here. This assumption yields:

$$I_6(t) = I_5(0,t) = I_o \left\{ \int_{x_o - st}^{x_o + w - st} \frac{\sin x''a}{x''} \cdot \frac{\sin x''a}{x''}\ dx'' \right\}^2$$

This integration can be done to yield:

$$I_6(t) = I_o \left\{ Si\, 2a(w + x_o - st) - Si\, 2a(x_o - st) - \frac{\sin^2 a(w + x_o - st)}{a(w + x_o - st)} + \frac{\sin^2 a(x_o - st)}{a(x_o - st)} \right\}^2$$

Again the reader should be cautioned that $x_o - st$ is a scaled distance. In fact, to compare the result with those previously present, the substitutions $aw = w$ and $-u' = a(x_o - st)$ should be made. In this case

$$I_6(t) = I_o \left\{ Si\, 2u' - Si\, 2(u' - w) + \frac{\sin^2(u' - w)}{u' - w} - \frac{\sin^2 u'}{u'} \right\}^2$$

the normalization constant is again chosen to be the intensity value at $u' = w/2$. For values of $w \geq 300$, the normalized intensity equation becomes:

$$I_6(u') = \frac{1}{\pi^2}\left\{\frac{\pi}{2} + Si(2u') - \frac{\sin^2 u'}{u'}\right\}^2 \qquad (25)$$

This function has been evaluated numerically and is shown in Figure 8 along with the curves for $\epsilon = 0.8$ and ∞ (incoherent limit) for comparison. An expanded scale is also shown in order to see the relative edge gradients more clearly. The narrow slit case is improved compared to the incoherent limit ($\epsilon = \infty$) with respect to contrast and edge gradient. In addition, there is an increase in the edge gradient compared to $\epsilon = 0.8$ case. Additional analysis is being made in the areas of increased illuminating slit width and increased scanning apertures.

RING SOURCE

A computer program for theoretical study of a ring source in a circular aperture has been written and tested in a trial run. It is anticipated that results will be presented in a later memo.

Future areas of investigation of partially coherent illumination will include continued theoretical study of the illuminating system under Project Microcap and the ring source problem under the Internal Research Program. Sine-wave objects will also be given a brief consideration. An experimental program designed to demonstrate the theoretical results, which has been delayed, will be started shortly.

STATINTL

[redacted]

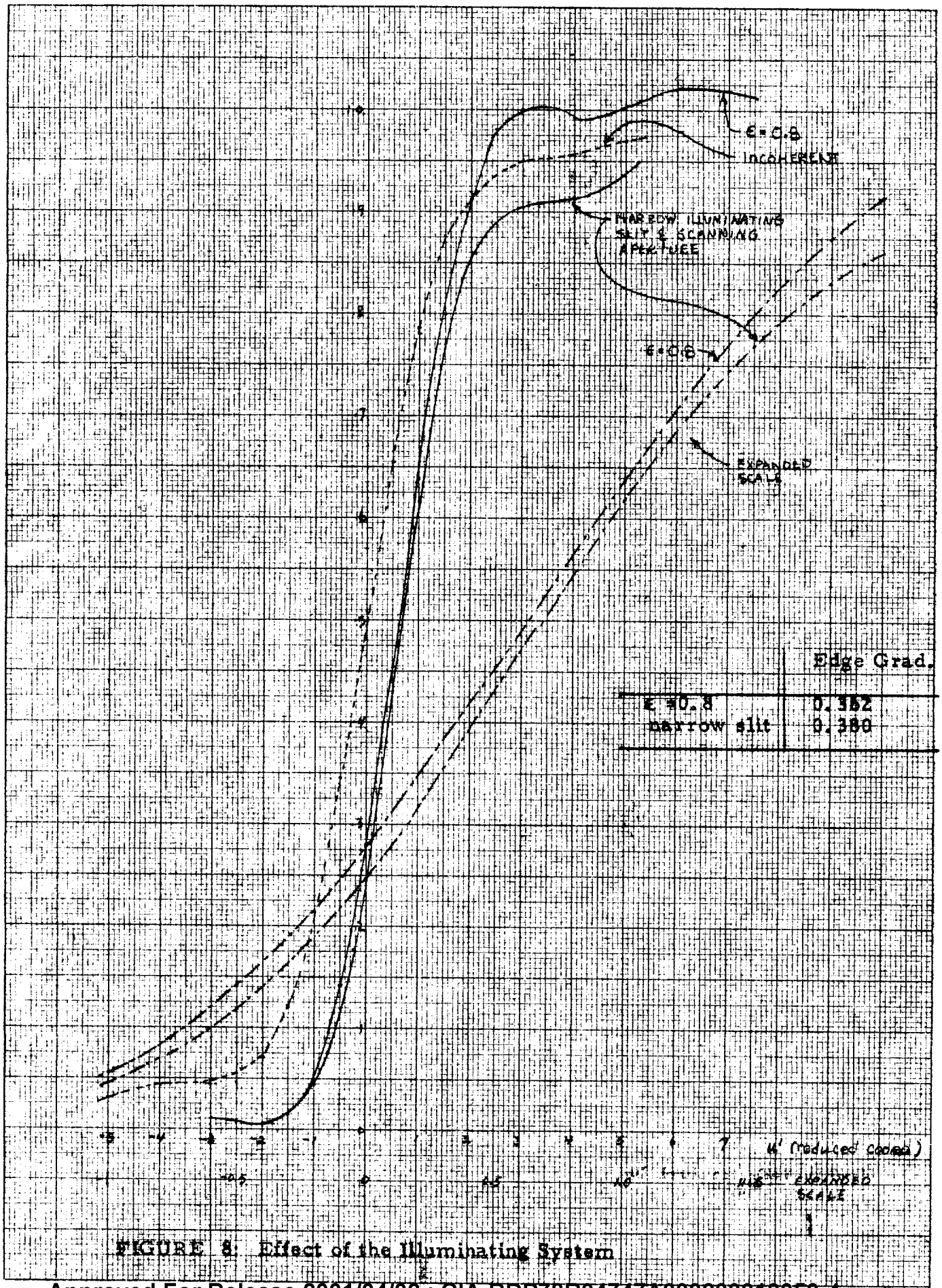

FIGURE 8: Effect of the Illuminating System